

# Investigation of Electropolymerized Polypyrrole Composite Film: Characterization and Application to Gas Sensors

N. V. Bhat,\* A. P. Gadre, V. A. Bambole

Physics Division, Department of Chemical Technology, University of Mumbai, Matunga, Mumbai, 400019, India

Received 10 October 2001; Accepted 6 May 2002

**ABSTRACT:** Polypyrrole–Polymethylmethacrylate (PMMA + PPy) composite films were prepared electrochemically by means of codeposition at constant potential. The films were characterized by using Infrared spectroscopy, wide-angle X-ray diffraction analysis, and scanning electron microscopy. The appearance of standard and some new absorption bands for PPy and PMMA confirms the composite formation. The mechanical properties of the conducting PMMA + PPy films were studied and found to be improved with respect to the control PPy films. The electrical conductivity of the PMMA + PPy film was measured by using standard

four- and two-probe methods. The conductivity of the films was found to depend on the pyrrole content. These conducting composites were further used as gas sensors by observing the change in the current when exposed to ammonia gas. The film gives a fast and reproducible response towards ammonia gas. © 2003 Wiley Periodicals, Inc. *J Appl Polym Sci* 88: 22–29, 2003

**Key words:** polypyrroles; composites; FTIR; mechanical properties; sensors

## INTRODUCTION

Recently, electrochemically polymerized conducting polymers have attracted lot of attention. Conducting polypyrrole film available via the electrochemical oxidation of pyrrole has been reported as electrode material.<sup>1,2</sup> Numerous studies for pyrrole-based conducting polymers have been reported by Bargon et al.<sup>3</sup> Comparing the electrochemically and chemically polymerized systems<sup>4–12</sup> the electrochemically prepared conducting polymers are relatively stable in air and the physico-chemical properties of the systems are not easily changed by an external stimulus. To improve the structural and electrical properties, the preference of composite materials containing a conducting polymer alloyed with a nonconducting polymer has been proposed. Conducting composites of polypyrrole (PPy) and a number of polymers used as matrices has been reported. Some of those matrix polymers used to prepare the composites are poly(vinylmethyl ketone),<sup>13</sup> poly(4-vinyl pyridine),<sup>14</sup> polyamide,<sup>15</sup> polycarbonate,<sup>16</sup> polystyrene,<sup>16</sup> PVC,<sup>17,18</sup> and PVA.<sup>19</sup>

Lindsey and Street<sup>20</sup> studied the PPy–PVA composite films prepared by electrochemical polymerization onto a precoated PVA matrix. These studies concluded that the composite films combine the advantageous mechanical properties of the host polymer with

the electrical properties of conducting polymer. However, it was pointed out<sup>20</sup> that the initial deposition of PPy occurred mainly at the precoated insulating matrix–electrode interface and led to the surface, rather than bulk, conduction of the composite film. It was observed that the conductivities on the electrode sides were generally more reproducible than on the solution sides of the composite films, where PPy was inhomogeneously deposited, and also this process is a sort of two-step process. Therefore, we opted a new approach to prepare a composite film through the electrochemical codeposition of a conductive polymer and the insulating polymer to prevent their inhomogeneous distribution.

In the present investigation an attempt has been made to prepare the composite materials containing conducting polymer (PPy) alloyed with another polymer (PMMA) and investigate its structural, mechanical, and electrical properties.

## Experimental

Pyrrole (99%) was obtained from Aldrich chemicals and was distilled before use. PMMA was obtained from Polyscience Inc., having the viscosity of 0.2; LiClO<sub>4</sub> was used as the supporting electrolyte, and was obtained from Across Organics; and Acetonitrile (AR Grade) was obtained from S.D.Fine Chemicals Ltd., having a molecular weight of 41.05.

PMMA + PPy films were prepared in potentiostatic conditions on a stainless steel electrode in a single compartment cell containing 0.1 M PPy, 0.1 M LiClO<sub>4</sub>, and 2% W/V PMMA in acetonitrile solution. The

Correspondence to: V. A. Bambole.

\*Now at Bombay Textile Research Association, Bombay-86, India.

counterelectrode was a graphite rod, and a saturated calomel electrode was used as a reference electrode. The electropolymerization was carried out using PARC 273 A Potentiostat/Galvonostat having the Run 270 software system. After electropolymerization the working electrode was dried at room temperature and rinsed with distilled water. The resulting flexible composite film was then easily removed from the electrode for structural and electrical conductivity measurements. The thickness of the films were determined by the thickness gauge (Model BAKER-MERCER type C-17.) SEM studies of the films coated with gold were performed by using Philips Scanning Electron Microscope (Model 515).

FTIR spectra of the samples were recorded on the Perkin-Elmer Spectrophotometer and was operated in normal slit, 10 min. scan mode. The X-ray diffraction patterns were recorded using a Phillips X-ray generator model PW 1729 and automatic X-ray diffractometer model PW 1710 unit.

Mechanical properties were measured using an Instron tensile tester model 1026. The conductivities of the free-standing PMMA + PPy films were measured by using a standard two-probe method. The dependence of the electrical conductivity of the PMMA + PPy films was measured over a temperature range from 303–353 K. The sample was placed in a chamber with a heating rate of 2–3°C /min, and the conductivity of the sample was recorded at each temperature.

## RESULTS AND DISCUSSION

### IR spectral analysis

The IR spectral analysis of pure PPy, pure PMMA, and the conducting PMMA + PPy composites are shown in Figure 1(a), (b), and (c), respectively. The IR spectra of pure polypyrrole [Fig. 1(a)] shows absorption near 1550  $\text{cm}^{-1}$  (—C=N and C=C ring stretching), 1050  $\text{cm}^{-1}$  (—NH bending deformation) and 950  $\text{cm}^{-1}$  (—CH out-of-plane bending). The IR spectrum of pure PMMA is shown in Figure 1(b). The absorption band at 3440  $\text{cm}^{-1}$  is due to the (C=O) group. The bands at 2994, 2950.8, and 2842.9  $\text{cm}^{-1}$  are present due to the combination of the ester  $\text{CH}_3$  group. The band appearing at 1735  $\text{cm}^{-1}$  was obtained with very strong intensity and is due to the (C=O) group. The absorption band appearing from 1272.1 to 1151.3  $\text{cm}^{-1}$  are due to the skeletal stretching. All these bands for IR spectrum of pure PMMA are in conformity with those reported in the literature.<sup>21</sup> The curve C of Figure 1 shows the IR spectrum of conducting composite of PMMA + PPy, which is somewhat similar to that for conducting Ppy. The relative intensities are, however, different.

An intercomparison of spectra in Figure 1(a) and (b) with Figure 1(c) makes it evident that the changes

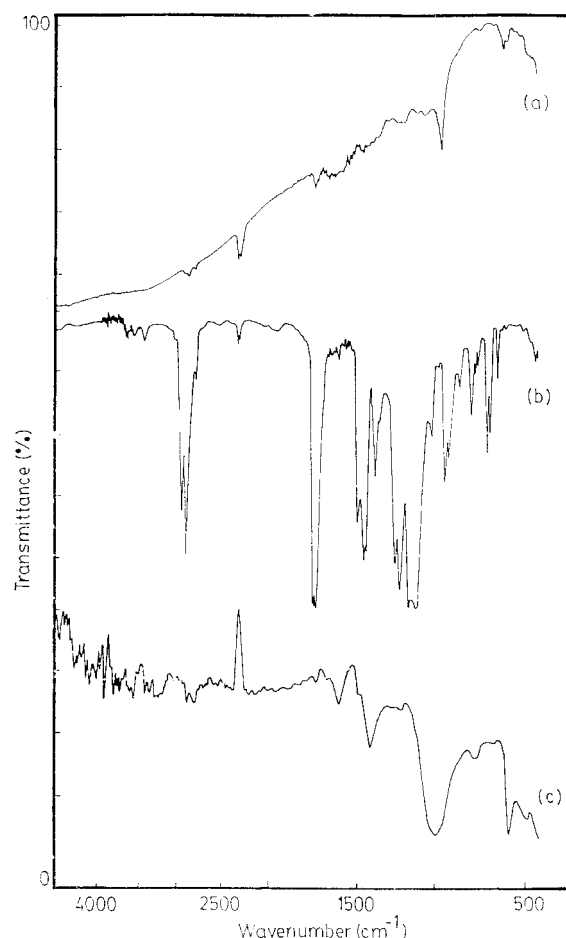


**Figure 1** Infrared spectra of (a) pure PPy, (b) pure PMMA, and (c) PMMA+PPy composite film.

are appreciable. Slight shift in bands are also observed at 3620, 1726, and 1484  $\text{cm}^{-1}$ . The intensity of band appearing at 1744  $\text{cm}^{-1}$  was found to be less compared to IR spectrum of the pure PMMA [Fig. 1(b)]. The presence of dominant bands for PMMA at 3617, 1744.1, 1640, and 1115.0  $\text{cm}^{-1}$  and absorption bands for PPy at 1659, 1458, and 1046  $\text{cm}^{-1}$  confirms the interaction between PPy and PMMA.

Comparative positions of different bands in the pure and composite material are given in Table I. Shift of the C=O band of PMMA from 1735 to 1726  $\text{cm}^{-1}$  is probably due to the interaction of hydrogen (H) from pyrrole molecule. A scheme of bonds is shown in Figure 2. Presence of "H" induces flexibility in the bond, and as a result the C=O bond starts vibrating at lower energy (hence, lower wave number). However, we do observe an additional peak at 1744  $\text{cm}^{-1}$ , which is due to overtone.

Similarly, the absorption band due to N—H bending of Ppy has shifted from 1050, to 1046  $\text{cm}^{-1}$ . Because the hydrogen atom is involved in bonding between "N" on one side and "O" on other side, the vibration should have been restricted and the absorp-

TABLE I  
Comparative Positions of Different Bands in the Pure and Composite Material

Functional Groups	PMMA $\text{cm}^{-1}$	PPy $\text{cm}^{-1}$	PMMA + PPy $\text{cm}^{-1}$
—CH out of plane bending		950	
—NH bending		1050	1046
Skeletal Stretching	1151.3–1272.1		1150
—C=N and C=C ring stretching		1550	1484,1458 1640,1659
C=O	1735		1726,1744
CH <sub>3</sub>	2842.9, 2950, and 3440 3617		3620,3617

tion should shift to higher energy side. However, the experimental observation of shift to the lower wave number is probably due to additional interaction of intra chain bonding and the presence of dopant molecule  $\text{ClO}_4^-$ .

### Wide-angle X-ray diffraction analysis

The Wide-angle X-ray Diffraction scans (WAXD) of pure PMMA, pure PPy doped with  $\text{LiClO}_4^-$ , and conducting PMMA + PPy composite films are shown in Figure 3(a), (b), and (c), respectively. Table II shows the angular positions ( $2\theta$ ), and the interplaner spacing ( $d$ ) values for pure PMMA, pure Ppy, and PMMA + Ppy, respectively. The XRD scan of pure PMMA [Fig.3(a)] shows an amorphous halo at  $2\theta = 13.4^\circ$ . This compares well with that reported in the literature.<sup>21</sup> XRD scan of Ppy with  $\text{LiClO}_4^-$  dopant shows about five peaks, which are superposed over a large increasing scattering background. The sharp peaks located at  $2\theta = 15.3^\circ$  and  $2\theta = 24.6^\circ$  do not compare well<sup>22</sup> with those reported in the literature. This is probably because of the  $\text{ClO}_4^-$  dopant ion. It was thought interesting to study the XRD of composite of PMMA + Ppy with  $\text{LiClO}_4^-$  dopant. Different composite films with electropolymerisation for 5, 10, and 20 min were prepared in potentiostatic modes at 1.2 volts [Fig. 3(c–e)]. The main feature of the XRD's for these three composites is occurrence of broad scattering halo centered around  $2\theta = 23^\circ$  and superposed with some sharp peaks. The sharp peaks observed for these three composites vary to some extent for their intensities as well

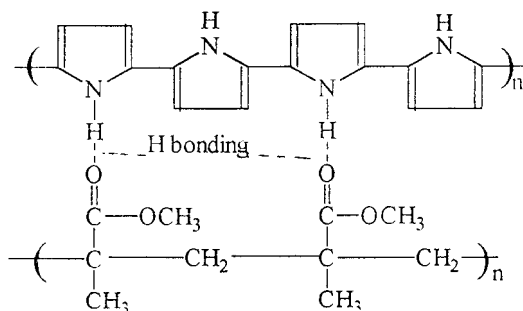


Figure 2 Scheme of bonds.

as locations. However, the common peaks observed for these scans are located at  $2\theta = 15.9^\circ, 23^\circ, 24.6^\circ, 27.4^\circ,$  and  $31^\circ$ . The sample prepared for 20 min, however, has the largest number of additional peaks. These peak positions compare partially well with our earlier work for PVDF + Ppy composite.<sup>23</sup> Detailed calculations are underway to determine the  $\{hkl\}$  indices and “ $d$ ” spacing and compare them with that reported in the literature. Earlier work has shown<sup>24</sup> two possible crystalline forms of Ppy, namely monoclinic and orthorhombic. In addition, work of Mitchell et al.<sup>25</sup> show the structure as a kind of interlayer spacing. In view of this and in view of many sharp peaks we observe, it is concluded that Ppy does crystallize to a large extent even in the presence of  $\text{LiClO}_4^-$  and PMMA. From the XRD scans it appears that the overall intensity of scattering increases with the time of polymerization and also some peaks become sharper. It must be mentioned that  $\text{LiClO}_4^-$  is highly crystalline, but none of the peak positions observed for the composites match with the peaks for pure  $\text{LiClO}_4^-$ .

### Morphological studies: SEM

The morphologic studies of the PMMA + PPy composites were carried out using SEM (Philips SEM 515). The morphology of the polymer depends mainly on

TABLE II  
 $2\theta$  and  $d$  Values for Pure PMMA, PPy,  
and PMMA + PPy Composite

PMMA		PPy		PMMA + PPy	
$2\theta$	$d$	$2\theta$	$d$	$2\theta$	$d$
11.4	7.76				
13.4	6.60				
14.6,15	6.06	15.3	5.79	15.2	5.82
	5.90			19.3	4.59
20	4.44	20.3	4.37	22.6	3.93
(shoulder)		24.6	3.61	23.8,24.6	3.73,3.61
				25.8	3.45
				27.4	3.25
		31	2.86	30.2,30.9	2.95,2.89
		32.1	2.78		
				34.6	2.59

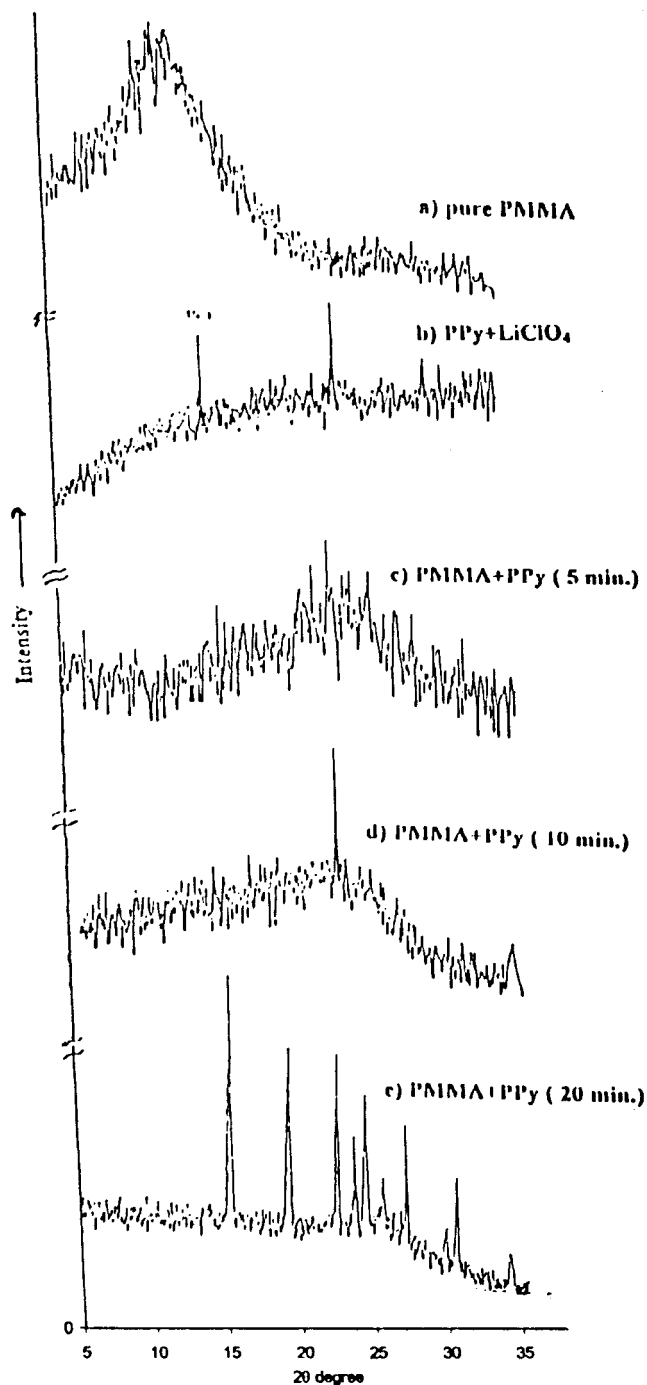
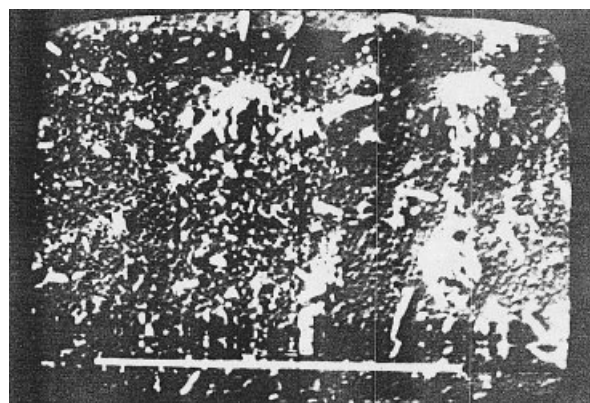


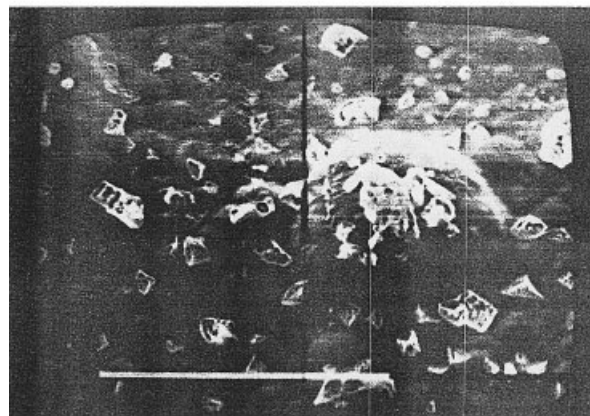
Figure 3 Wide angle X-ray diffraction spectra of (a) pure PMMA, (b) pure PPy, and (c) PMMA+PPy composite film.

the structure of the monomer, nature of the dopant, and the thickness of the polymer film grown on the electrode. Figure 4(a), (b), and (c) shows the electron micrographs of PMMA + PPy composite films for various polymerization time such as 5, 10, and 20 min, respectively. The films prepared under different conditions show the globular structures of PPy in the PMMA matrix, which is smooth and relatively homogenous in appearance. As the time of polymeriza-

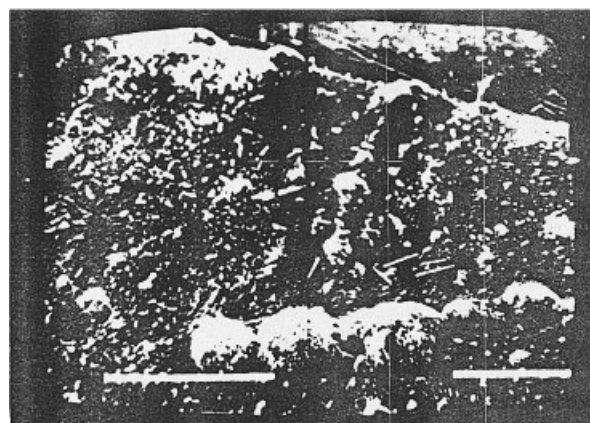
tion was increased from 5 to 10 min, the average size of globules increased and those could be seen distinctly. Further increase in the time of polymerization to 20 min shows that the number of globular structures of PPy increased and formed a chain-like pattern



(a)



(b)



(c)

Figure 4 Scanning electron micrograph of PMMA+PPy composite films. (a) PMMA+PPy composite film for 5-min growth; (b) PMMA+PPy composite film for 10-min growth; (c) PMMA+PPy composite film for 20-min growth.

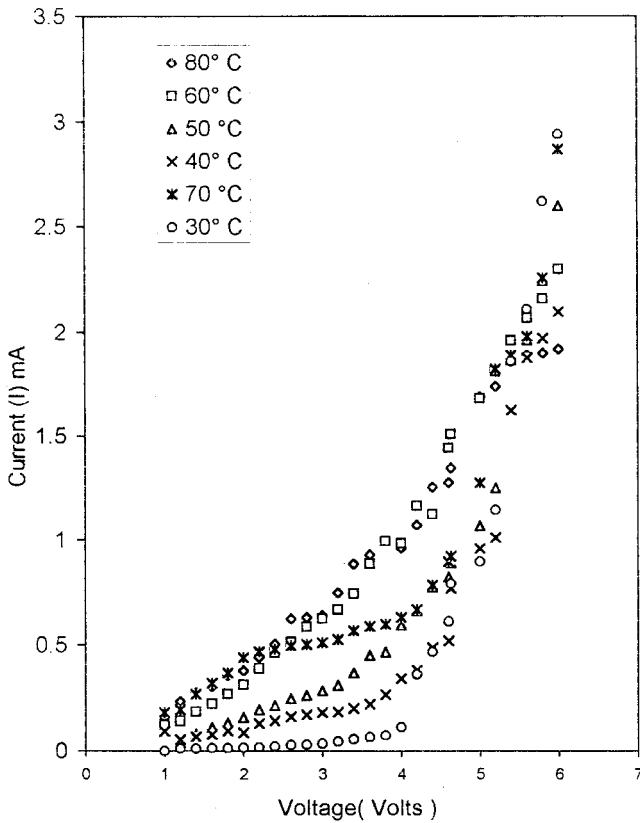


Figure 5 Current (I) - Voltage (V) characteristics of PMMA + PPy composite films.

in the homogenous PMMA matrix. The average size of the globules was found to be 12  $\mu\text{m}$ .

**Mechanical properties**

Tensile strength for pure PPy film and pure PMMA was found to be 32.4 and 49.0 Mpa, respectively. This compares well with the values reported in the literature.<sup>23</sup> It was observed that the tensile strength of conducting composite film of PMMA+PPy film is 82.86 Mpa. Thus, mechanical properties of PPy films were found to have been improved by the formation of composite with PMMA.

**Electrical conductivity measurements**

The current voltage characteristics of PMMA + PPy composite films at various temperatures (303 °K to 353 °K) was studied. It was observed that the I-V characteristics of these films are nonlinear, indicating the nonohmic behavior of the samples (Fig. 5). Assuming that the normal energy band picture can be applied to an insulating thin film, there would appear to be six possible separate conduction mechanisms. Testing of the observed data for various mechanisms was carried out by assuming certain basic relations during the

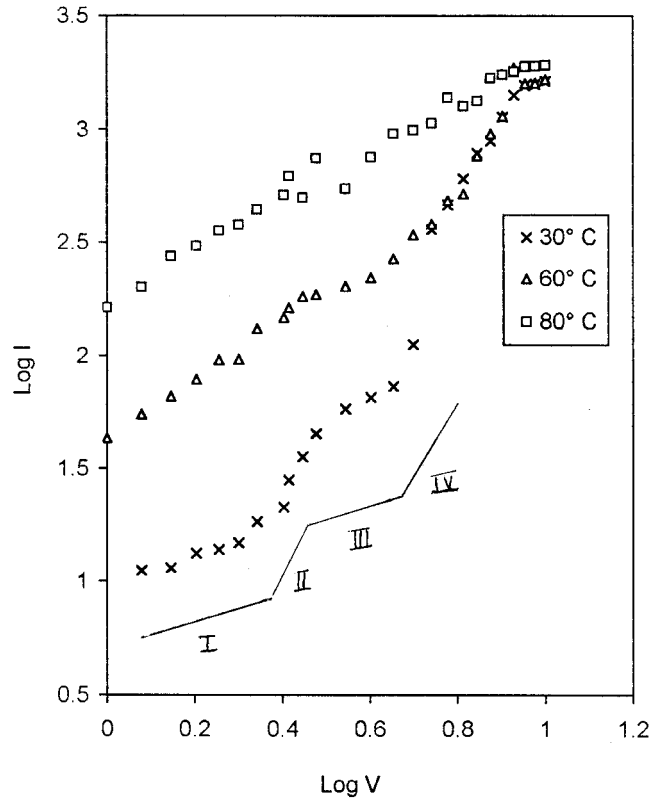


Figure 6 Log current (I) - log voltage (V) characteristics of PMMA + PPy composite films.

analysis. The data was plotted as  $\log I$  vs.  $\log V$ ,  $\log I$  vs.  $\log I/T^4$ ,  $\log \sigma$  vs.  $1/T$ . Analysis of such plots revealed that the mechanism of ionic, Schottky and Poole Frenkle emission, hopping, impurity conduction can be ruled out. Therefore, it is most likely that the current is limited due to space charge (Fig. 6). From the general nature of plot of  $\log I$  vs.  $\log V$  and the slopes in low and high voltage regions it seems that SCLC is the main mechanism of conduction but is dominated by traps. A close look shows four regions I to IV, but the increase in the slopes is not ideal. There is rapid decrease in the slope in region III, although slope in region IV is more than 2. The decrease of slope indicates the presence of a large number of shallow and deep traps. On this basis we suggest a band-like

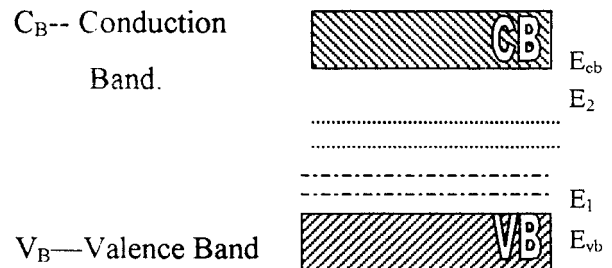


Figure 7 Band-like model.

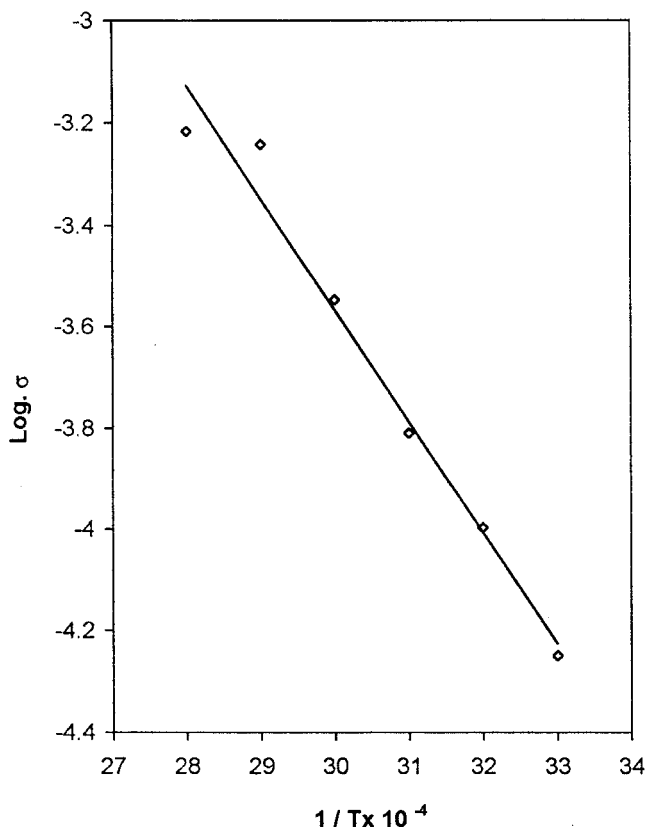


Figure 8 Log conductivity ( $\sigma$ ) -  $1/\text{temperature}$  ( $T$ ) characteristics of PMMA + PPy composite films.

model (Figure 7) with traps very near the top of valence band and just below the bottom of the conduction band.

It was thought interesting to find why slope in region III departs from ideal SCLC and therefore I-V and  $\log I$ - $\log V$  data for pure PMMA was analyzed. It was seen that although PMMA is a good insulator, the data of  $\log I$ . vs.  $\log V$  does indicate similar behavior.

To study the variation of conductivity ( $\sigma$ ) with temperature, the plots of  $\log(\sigma)$  vs. reciprocal of absolute temperature were obtained for conducting PMMA + Ppy film as shown in Fig. 8.

The calculation of  $\sigma$  was made on the basis of I-V plot shown in Figure 5. Because this plot is nonlinear, it is evident that region from 0-4 V can be considered as "low field" and 4-10 V can be considered as high-field regions. An illustrative graph for  $\log \sigma$  vs.  $1/T$  for "low fields" is shown in Figure 8. It may be seen that there is a sharp increase in conductivity when temperature was raised from 303 to 353 °K. Therefore, the average slope of the straight line was obtained. The activation energy calculated on the basis of this slope was found to be 0.08 eV. This low value of activation energy indicates that the mode of conduction is electronic.

### Response to $\text{NH}_3$ gas

The recent emergence of concern over environmental pollution and efficiency in a variety of processes and increased awareness over a need to monitor potentially hazardous gases has stimulated substantial research and development in the field of gas sensors. These gases include CO,  $\text{CO}_2$ ,  $\text{NO}_2$ ,  $\text{NH}_3$ , etc. Thus, the design, fabrication, and application of novel amperometric, chemical, and biologic sensors has been a topic of considerable interest in recent years.<sup>26,27</sup> This research activity has occurred in tandem with rapid developments in the area of polymer modified electrodes.<sup>28</sup> The polypyrrole-based polymer is operated under conditions where it is electronically conducting, and by suitable choice of the dopant concentration during electropolymerization, one can obtain a polymer-modified electrode that exhibits a minimal pseudocapacitive background current. The latter is a very desirable property from the analytical view point, in that the sensor may be readily used to determine absorbate at the micromolar levels.

The objective of this article is not only to study the structural and electrical properties of conducting polymer composites but also to pursue the developing

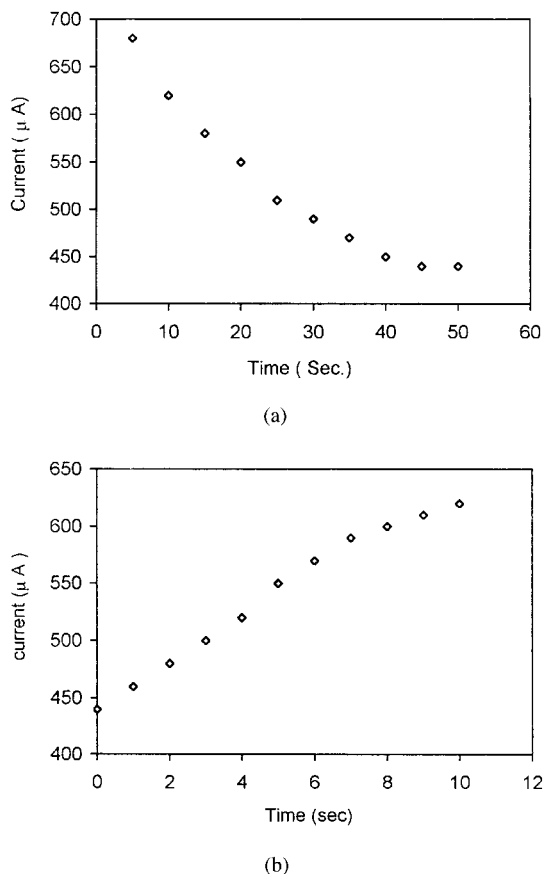
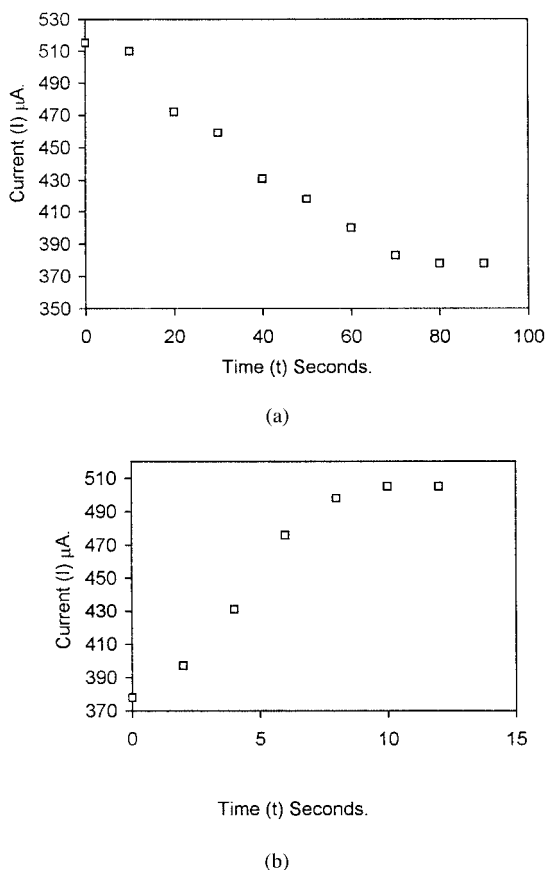


Figure 9 (a) PMMA + PPy composite films when exposed to 100% ammonia gas (gas in). (b) PMMA + PPy composite films when exposed to air (gas out).

field of the gas sensors, with special emphasis on those based on the polymeric materials, for toxic gases such as ammonia, and to analyze the performance and basic working principles of these sensors.

In the present investigation we have synthesized the composites of PMMA+PPy, and therefore, it was thought to be interesting to test these materials for sensing gases. The composite film was placed in the test chamber and the test chamber was evacuated. When ammonia 100% was allowed to flow in, it was noticed that there is a sudden decrease in the current which is about  $240 \mu\text{A}$ , and the change was brought in 50 s [Fig. 9(a)]. When the gas was desorbed the current started increasing and reached its steady value of  $680 \mu\text{A}$  in about 10 s [Fig. 9(b)]. It was decided in the next set of experiments to find the sensitivity of the material, and therefore, the percentage of the ammonia flowing in the test chamber was decreased to (0.1%) (w.r.t.  $\text{N}_2$  in the mixture). Even in this case the response was quite fast but the total change in the current was slightly less than  $240 \mu\text{A}$ . The graphical representation of the response with respect to time is shown in [Fig. 10(a)]. When the composite film was exposed to ammonia gas (0.1%) it can be observed that the decrease in the current is about  $160 \mu\text{A}$ , and the



**Figure 10** (a) PMMA + Ppy composite films when exposed to 0.1% ammonia gas. (b) PMMA + Ppy films when exposed to air.

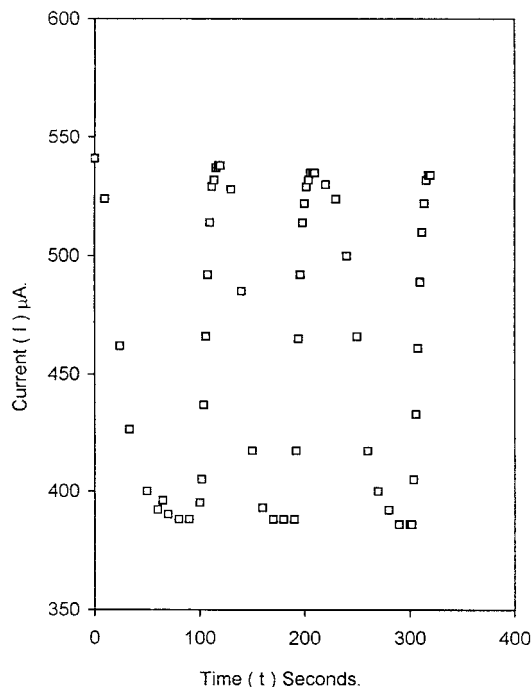
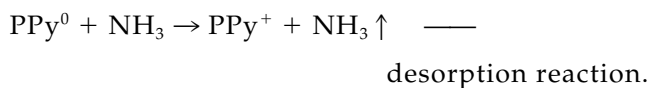
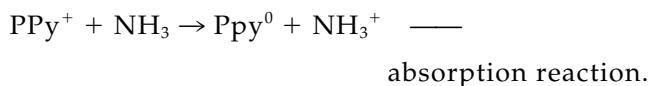


**Figure 11** Cyclic behavior of PMMA + PPy composite films treated with ammonia gas.

change was brought in less than 50 s. When the gas was desorbed, the current again started increasing and reached its steady value of  $500 \mu\text{A}$  in about another 12 s [Fig. 10(b)]. Figure 11 also shows the cyclic behavior when the gas is in (absorption) and when the gas is out (desorption). Thus, the composite film showed fast and reversible current variation response against ammonia gas. The decrease in the current on the exposure to ammonia gas can be understood from the fact that the nitrogen contains a lone pair of electrons which can be donated to the initially oxidized polypyrrole. This will neutralize the PPy cation (+charge) and, therefore, the number of carriers will decrease, resulting in the decrease of the current.

This reaction can be represented by



The desorption of gas by vacuum or by bringing the test chamber to the normal air results in the reformation of  $\text{PPy}^+$ , and therefore, the current increased to the steady-state level. In the previous experiments in our laboratory, it was reported that the neutralized films show much better response. On the basis of these results it was concluded that the vacant sites and

porosity in the film are necessary for increased sensitivity.

## References

1. Street, G. B.; Clark, T. C. *IBM J Res Dev* 1981, 25, 51.
2. Baughman, R. H.; Bredas, J. L. Charles, R. R.; Elsenbaumer, R. L.; Schacklette, L. W. *J Chem Rev* 1982, 82, 209.
3. Bargon, J.; Mohmad, S.; Waltman, R. J. *IBM J Res Dev* 1983, 27, 330.
4. Diaz, A. F.; Castillo, J. B.; Logan, J. A.; Lee, W. Y. *J Electroanal Chem* 1981, 129, 115.
5. Burgmayer, P.; Murray, R. W. *J Am Chem Soc* 1982, 104, 6139.
6. Pfluger, P.; Krounbi, M.; Street, G. B. *J Chem Phys* 1983, 78, 3212.
7. Choi, K. M.; Jang, J. H.; Kim, K. H. *Mol. Cryst Liquid Cryst* 1992, 220, 201.
8. Choi, K. M.; Lee, E. J.; Park, J. W.; Kim, K. H.; *J Appl Polym Sci* 1991, 42, 2129.
9. Choi, K. M.; Kim, C. Y.; Kim, K. H. *J Phys Chem* 1992, 96, 3783.
10. Choi, K. M.; Kim, K. H. *J Appl Polym Sci* 1992, 44, 751.
11. Kong, S.; Choi, K. M.; Kim, K. H. *J Phys Chem Solids* 1992, 53, 657.
12. Choi, K. M.; Jang, J. H.; Rhee, H. W.; Kim, K. H. *J Appl Polym Sci* 1992 46, 1695.
13. Wang, H. L.; Fernandez, J. E. *Macromolecules* 1992, 25, 6179.
14. Mohammadi, A.; Lundstorm, I.; Inganas, O.; Salaneck, W. R. *Polymer* 1993, 395, 31.
15. Tieke, B.; Gabriel, W. *Polymer* 1990, 31, 20.
16. Wang, H. L.; Toppa, L. Fernandez, J. E.; *Macromolecules* 1990, 23, 1053.
17. Niwa, O.; Tamamura, T.; *J Chem Soc Chem Commun* 1984, 817.
18. De Paoli, M. A.; Waltman, R. J.; Diaz, A. F.; Bargon, J. J. *Chem Soc Chem Commun* 1984, 1015.
19. Makhlouki, M.; Morsli, M.; Bonnet, A.; Conan, A.; Paron, A.; Lefrant, S. *J Appl Polym Sci* 1992, 44, 443.
20. Lindsey, S. E.; Street, G. B.; *Synth Met* 1984, 10, 67.
21. Street, G. B. In *Handbook of Conducting Polymers*; Skotheim, T. A. Ed.; Marcel Dekker: New York, 1986, p. 280, vol. 1.
22. Baunman, U.; Schreiber, H.; Tessmar, K.; *Macromol Chem* 1960, 36, 81.
23. Geeta, P. Ph.D Thesis, University of Mumbai, 1999.
24. Kusy, R. P. *J Polym Sci Polym Chem Ed* 1976, 14, 1521.
25. Mitchell, G. R.; Geri, A. *J Phys D Appl Phys* 1987, 20.
26. Borman, S. *Anal Chem* 1987, 59, 1091A.
27. Albey, W. J.; Bartlett, P. N.; Cass, A. E-G.; Craston, D. H.; Hagget, B. G. D. *J Chem Soc Faraday Trans I*. 1986, 82, 1033. (Special issue" New Electrochemical Sensors).
28. Hillman, A. R. In *Electrochemical Science and Technology of Polymers*; Linford, R. G., Ed.; Elsevier:Amsterdam, 1987, p. 103.